



Simulation of rainfall–runoff process for an ungauged catchment using an event-based hydrologic model: A case study of koraiyar basin in Tiruchirappalli city, India

SURENDAR NATARAJAN*  and NISHA RADHAKRISHNAN

Department of Civil Engineering, National Institute of Technology, Tiruchirappalli, Tiruchirappalli 620 015, India.

**Corresponding author. e-mail: suredarnatarajan86@gmail.com*

MS received 20 February 2020; revised 30 September 2020; accepted 28 October 2020

The Koraiyar River basin is located in Tiruchirappalli city, one of the fastest-growing medium-sized cities in south India. Over the decades, the city has experienced sporadic flooding in vast areas due to the breaching of bunds when the river is in spate. The objective of this investigative study is to simulate rainfall–runoff in the Koraiyar basin watershed through the reliable Hydrologic Modelling System developed by the Hydrologic Engineering Center (HEC-HMS). Land-use and land-cover constantly change due to increasing population taken as one of parameter, its influence on CN, and their impact on surface runoff is analyzed in this study. The specified hyetograph method is adopted for the meteorological modelling; the Soil Conservation Services-Curve Number (SCS-CN) is selected to calculate the loss rate, and the SCS unit hydrograph method is adopted to simulate the runoff rate. Calibration and validation of the model are done to simulate assessed peak discharge values for comparison with actual observed values. The Nash–Sutcliffe efficiency coefficient is between 0.5 and 0.6, which indicates that the hydrological modelling results are satisfactory and acceptable for simulation of rainfall–runoff. The peak discharge is obtained for the single maximum rainfall event of about 100 mm in a day over the past 40 years, and hydrographs are generated.

Keywords. Flood; land-use/land-cover; HEC-HMS; SCS; curve number; Koraiyar.

1. Introduction

Flood is the peak stage of water flow that exceeds or overtops natural or artificial channel (Dhruvish and Prashant 2013; Yucel 2015; Zope *et al.* 2015; Matej and Jana 2016; Mehdi *et al.* 2018; Aryal *et al.* 2020). Flood risk analysis is an important component of risk management (Zaharia *et al.* 2015). Analysis of extreme events like severe storms, floods, droughts is an essential component of hydrology and hydroclimatology (Maity 2018). Heavy rainfall events in an urban area stance

various challenges to the water resource managers in terms of flood mitigation, inundation, water conservation and harvesting for drinking water supply (Anandharuban *et al.* 2019). It occurs either due to prolonged heavy rainfall or short duration of extreme rainfall intensity, and both are characterized by peak stage discharge. Flooding leaves in its wake widespread infrastructural destruction, damages to dwellings, landslides, loss of human life, and other collateral hazards (Hapuarachchi *et al.* 2011). The study conducted by the UN Office for Disaster Risk Reduction (UNISDR) and the

Belgian-based Centre for Research on the Epidemiology of Disasters (CRED) shows that between the years 1995 and 2015, there were 3062 flood disasters that accounted for nearly 43% of natural disasters along with hazards such as earthquakes and volcanoes. Floods are ranked first in the world's natural disasters, causing nearly 42 million people of the world's population to be affected (Apel *et al.* 2009).

To predict flood intensity and to estimate water volume, a suitable modelling technique is required for flood management and reduction (Bates 2004). Hydrological modelling can reproduce the behaviour of a watershed during any rainfall event, and it helps to understand natural phenomena such as flash floods. It stimulates the natural hydrological processes that lead to the eventual transformation of rainfall into runoff (Ali *et al.* 2011; Pawan and Jayantilal 2018). The rainfall–runoff model establishes the quantum relationship between rainfall and runoff, and it helps in identifying the runoff rate from a river or canal when the input is given as rainfall intensity. The development of infrastructure projects and the design of drains, canals, and other channels depends on the volume of runoff that is generated and can be safely handled from rainfall in the concerned basin. The rainfall–runoff model is used to generate a hydrograph, which shows the variation of flow rate concerning the runoff from the basin outlet. The hydrograph generated is integrated with other software for studying urban storm water drainage, flood forecasting, and long-term safety measures for damage reduction (Zhang *et al.* 2013).

In recent years, inevitable changes such as increased land-use and reduced land-cover and their impacts on water resources and floods have been studied by hydrologic modelling (Yang *et al.* 2012). Several rainfall–runoff models like Mike and SWMM are available to estimate runoff volume and peak flow characteristics for proper hydrological modelling of a basin. The selection of the model depends on the hydrological simulation process and the availability of full data for the basin. Tung and Mays (1981) developed a non-linear hydrological system-state variable model to simulate urban rainfall–runoff and studied the variation of each parameter for different levels of urbanization. Bhaskar (1988) adopted Clark's instantaneous unit hydrograph concept to determine the parameters that influence the effect of urbanization on a watershed.

Ferguson and Suckling (1990) used regressive polynomial equations in impervious surfaces to

analyze the relationship between rainfall and runoff. Huang *et al.* (2008) used regression analysis to establish the relationship between hydrograph parameters and peak discharge, and their corresponding imperviousness to the urbanization of the Wu-Tu watershed in Taiwan. Cheng and Wang (2002) developed a method to define the degree of change in runoff hydrographs and evaluate the hydrological impacts of urbanization of the Wu-Tu watershed.

The development of the hydrological model and its application in rainfall–runoff processes have been done over the past decades (Jakeman and Hornberger 1993). The hydrological models can be classified into four main categories, namely, determinist or stochastic, semi-distributed, kinematic or dynamic, and empirical or conceptual. The empirical equations cannot be applied for large watersheds and long-term rainfall due to parameters such as curve number and runoff volume, as an estimation of time to reach a peak rate of runoff becomes challenging in large watershed areas (Onusluel *et al.* 2010; USACE 2013; Ismail 2015).

In hydrologic modelling, the calibration and validation processes require a large number of spatial and temporal data, but in practice, the data availability is scarce, and that must be managed (Kim and Choi 2015). The rainfall–runoff modelling is classified into two types: event-based and continuous models based upon its application. The event-based modelling deals with basin characteristics by using initial conditions from single rainfall events; a continuous model usually requires a longer time-step and is chosen for continuous hydrological modelling.

Estimation of runoff from ungauged basin is very important for the planning of water resource projects in the river basin (Khatri *et al.* 2018). Nowadays, watershed models are developed conceptually for the entire basin area to model the rainfall–runoff process (Madsen 2000). A significant challenge is the accurate prediction of catchment runoff responses to rainfall events. Hydrologic models help in better development and proper management of water and land resources (Zafar and Zaidi 2015). Several factors are responsible for choosing model features such as rainfall characteristics, watershed properties, and stream monitoring observations.

In the present study, the conceptual approach is adopted for the hydrologic modelling by using a semi-distributed hydrologic model of HEC-HMS (Hydrologic Engineering Center-Hydrologic

Modelling System) developed by US Army Corps of Engineers (USACE 2008). The HEC-HMS is a rainfall–runoff model that has both lumped and distributed parameter-based modelling (Komuscu and Celik 2012). The model has several options for simulating rainfall–runoff processes in basins. It is capable of simulating the rainfall–runoff relation of the dendritic watershed in space and time (Eyad and Broder 2013). This model is effectively used in different river basins for catchment modelling (Yusop *et al.* 2007). Sintayehu (2015) studied the HEC-HMS model by adopting the Snyder unit hydrograph and exponential recession method to simulate the runoff in the upper Blue Nile River basin. In Najran city, Kingdom of Saudi Arabia, Ismail (2015) modelled rainfall–runoff relations by HEC-HMS in an arid environment. Sampath *et al.* (2015) modelled the rainfall–runoff relations using HEC-HMS in the tropical catchment in Sri Lanka. Onusluel *et al.* (2010) employed the HEC-HMS to simulate rainfall–runoff in the urban region of Izmir, Turkey. Laouacheria and Mansori (2015) used the HEC-HMS model by employing a frequency storm to simulate the runoff in a small urban catchment. From these studies, a suitable framework is adopted for this study.

In this study, HEC-HMS 4.0 is used for developing a hydrologic modelling system for the Koraiyar River basin. For developing the model, the SCS Curve Number method is used in the distributed loss method, and in the transformation process, the SCS unit hydrograph method is used for determining the rainfall–runoff process. The Muskingum method is adopted for channel routing. The 16 maximum single rainfall events of rainfall more than 100 mm that occurred in the time range of 1977–2016 are taken for simulation and calibration of the rainfall–runoff process in the basin. After the calibration process, the model is validated from the years 2000–2013 after the extreme event year 1999 of maximum single rainfall event. Finally, the basic sensitive parameters that influence the runoff are identified from the simulation.

2. Study area description

The Koraiyar River and its catchment lie between the latitude $10^{\circ}32'40.24''$ – $10^{\circ}48'16.81''$ N and longitudes of $78^{\circ}32'23.94''$ – $78^{\circ}39'48.58''$ E in Tiruchirappalli city region, India. The Koraiyar River originates from the Othakkadai Karupur Redipatti

hills in Manaparai taluk of Tiruchirappalli district and finally flows into Uyyakondan channel in the center of the Tiruchirappalli city, Tamil Nadu, as shown in figure 1. The city has a subtropical climate. There is no significant temperature variation between summer and winter, with summer (March–May) having an extreme temperature of 41°C and a minimum of 36°C ; winter (December–February) generally being warm but pleasant with temperature ranging from 19°C to 22°C . Hot, humid, dry summers and mild winters are the main climatic features of the city. The rainy season that falls between October and December brings rain mostly from the northeast monsoon. The river flows through Manaparai, Thuvankurichi, and Viralmalai; the total length of the main river is 75 km, with a catchment area of 1498 km^2 . The average annual rainfall for the Koraiyar urban catchment is around 757.40–866.70 mm. The surplus water flows through Puthur weir outlet in the left bank of the Uyyakondan River and traverses Kodamurutty river for a length of 6 km before finally falling into the Bay of Bengal. The rain gauge stations in the basin are located at Marun-gapuri, Manaparai, and Trichy Airport.

3. Methodology adopted in study

The methodology adopted for the present study, shown in figure 2, is explained as below.

3.1 Data map preparation

Spatial and temporal data are required for the study. The temporal data of the maximum single rainfall event is collected from State Ground and Surface Water Resources Data Centre, Chennai. The spatial data is extracted using ArcGIS software. The spatial data like basin map, soil map, land-use land-cover, and CN map are generated. The data generated from the maps is given as input to the model. Sixteen single maximum rainfall events of the basin are selected for model simulation. The SCS method is used for determining the rainfall–runoff process. The SCS CN method implements the curve number methodology to calculate the amount of runoff from the precipitation. The maximum retention and catchment characteristics are connected through the curve number. The CN is taken as a weighted value based on different land uses in the study area. The

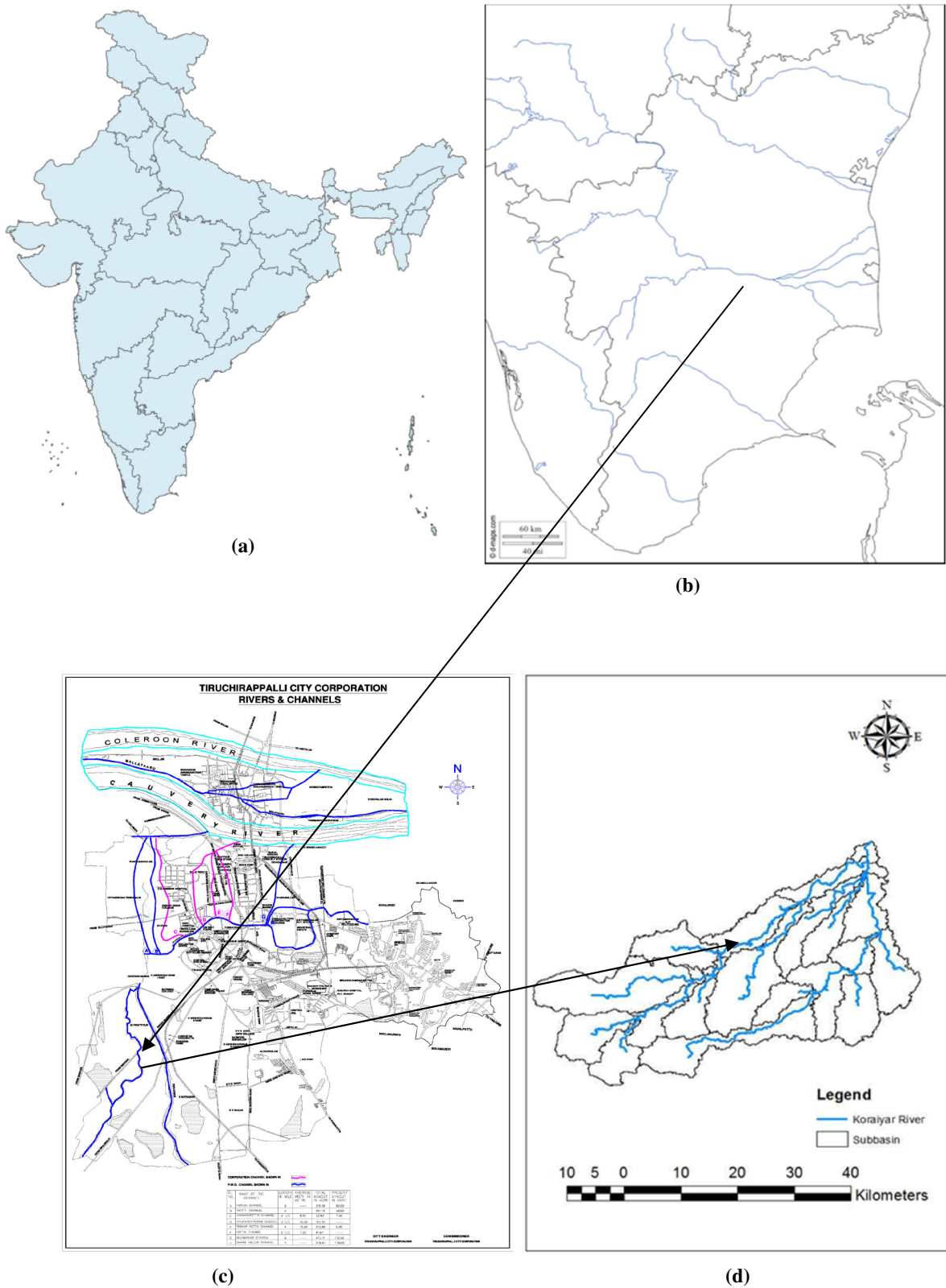


Figure 1. Study area. (a) Political map of India. River boundaries map of (b) Tamil Nadu, (c) Tiruchirappalli City Corporation, and (d) Koraiyar basin map.

control specifications are used to run the model for an event simulation, and it is used to define the time intervals for simulating rainfall events. The

Muskingum routing is used in each reach. The output of the model is the discharge hydrograph at each sub-basin outlet.

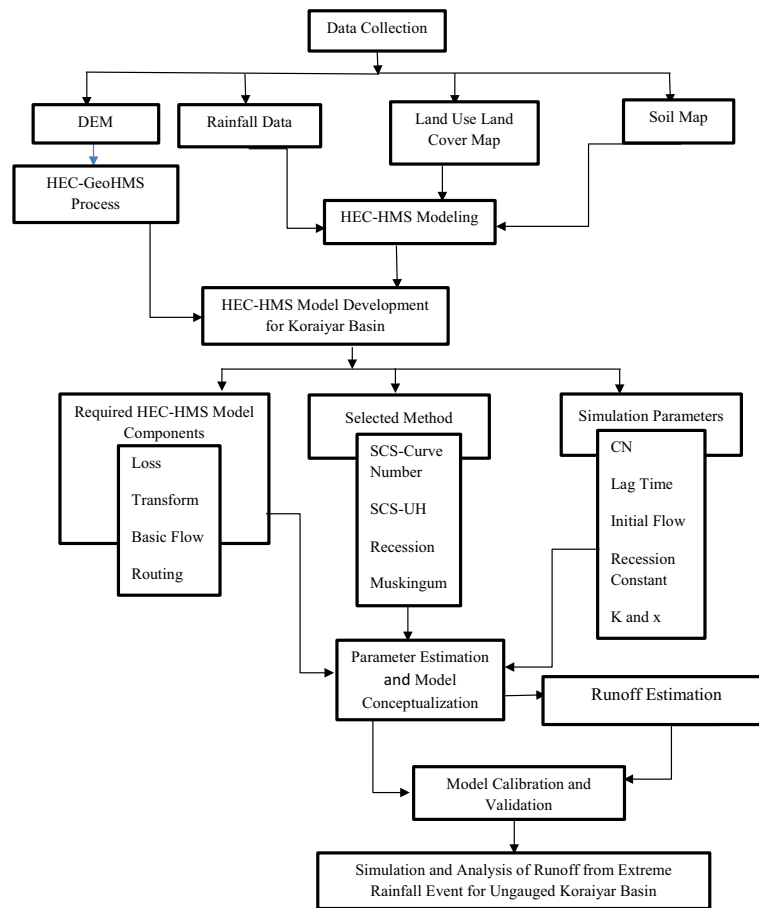


Figure 2. Framework of the study adopted for simulating rainfall–runoff process.

3.2 Development of hydrological soil map

The soil map for the Koraiyar basin extracted from the Food Agricultural Organization (<http://www.fao.org/soils-portal>) website in Harmonized World Soil Database v 1.2. is shown in figure 3. The predominant soil in the basin is red sandy soil indexed in HSG (A), which covers 16.05% of the total area in the basin. Mixed alluvium sandy loam and loamy soil are found in many sections of the delta areas near the Cauvery River (Suribabu and Bhaskar 2015; Surendar and Nisha 2019). The soil is brown to black, very deep loamy (C) with subtle texture, and covers about 4.93% of the total geographical area. The grey soil is distributed to about 12% of the entire basin. Black soil is observed in the northern parts and Ayacuts near the big tank and covers almost 14% of the total area in the basin. The other types of soil, like clay (D) and red ferruginous, are widely distributed throughout the basin. As per the US Natural Resource Conservation Service (NRCS), the hydrologic soil groups in the study area are classified as A, which has low runoff potential and high water transmission rate.

The group C type soil present in the basin indicates moderate infiltration and a slow transmission rate. The D type of soil present in the basin has high runoff potential and low water rate transmission.

3.3 Land-use land-cover

The land-use land-cover (LULC) of the study area is prepared from Landsat 7 ETM+ image of 30 m resolution for the year 2016, as shown in figure 4. Based on the NRSA classification for Indian conditions, the entire land is divided into agricultural land, built-up area, open land, vegetation, and water bodies (NRSA, Reddy 2002). It is classified using a maximum likelihood technique, which is a supervised classification method (Lillesand and Kiefer 2003; Suribabu *et al.* 2012). The LULC for the year 2016 is analyzed by using ArcGIS software. From the analysis, it can be noted that the agricultural land covers around 16% of the whole basin, and the dominant land use category is vegetation, which occupies over 16.93%. In the basin, open land comprises of around 7.57% of the whole area, while water bodies occupy the remaining area of 6.5% along with

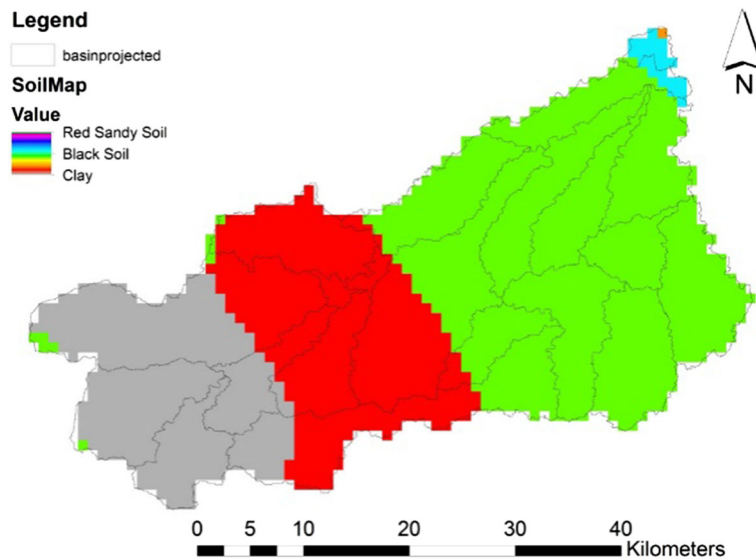


Figure 3. Soil map of the Koraiyar basin.

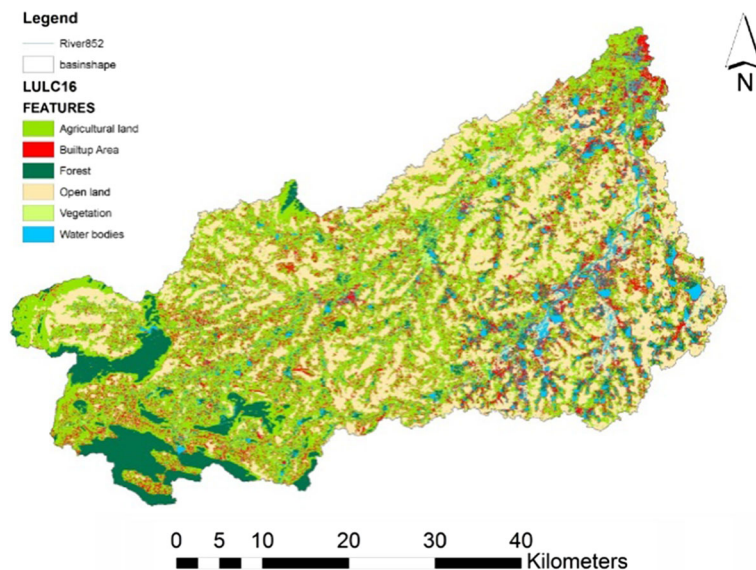


Figure 4. Land-use land-cover map of Koraiyar basin.

forest cover of 0.23%. From the analysis of LULC, it is noted that the built-up area in the basin shows the imperviousness corresponding to land use in the study area. Based upon the land-use conditions existing in different basins, they have respective percentage values of 0.5, 0.6, and 0.8. The average of imperviousness is taken between 0.5 and 1%, and it is calculated by processing land-use data in ArcGIS.

3.4 Developing rainfall–runoff model for the basin

The rainfall–runoff model for the study area is developed by incorporating an Arc-GIS 10.2.2 with

HEC-GeoHMS tool which uses SRTM image. The SRTM image is processed, where the basin and the entire hydrologic network is created as a basin file format for importing into the HEC-HMS model 4.0.2 (Knebla *et al.* 2005; Xuefeng and Steinman 2009; Azama *et al.* 2017). The geospatial database such as slope, basin centroid, and elevation, the stream length, and the longest flow path for each sub-basin is generated and projected to the WGS 1984 coordinate system. The rainfall amount of maximum single event for a day over a period of time is simulated by HEC-HMS. The Digital Elevation Model (DEM) of 30 m resolution is downloaded from Shuttle Radar Topographic Mission (<http://srtm.csi.cgiar.org>). The stream networks

and sub-basins are generated by processing the DEM in HEC-GeoHMS. The basin’s stream length, slope, longest flow path, length, the position of sub-basin centroid, elevation, and stream path are generated from the DEM, as shown in figure 5. The SCS unit hydrograph method is used to find the rainfall–runoff process (Lastra *et al.* 2008).

3.5 HEC-HMS Model

The Hydrologic Engineering Centre-Hydrologic Modelling System is used to simulate the rainfall–runoff process in the basin. It was developed by the US Army Corps of Engineers (Scharffenberg and Fleming 2010). The model arrangement consists of four main modules, namely, basin, meteorological model, control specifications, and input data in the form of time-series, paired data, and gridded data. Different methods like the deficit and constant, exponential, Green and Ampt, initial and constant, SCS curve number, Smith-Parlange, and Soil Moisture Accounting (SMA) are used for simulating the infiltration losses. For transforming excess precipitation into the surface runoff, methods like Clark unit hydrograph, kinematic wave, ModClark, SCS unit hydrograph, Snyder unit hydrograph, user-specified graph, and user-specified unit hydrograph are used. In HEC-HMS, routing models like kinematic wave routing, lag routing, modified puls routing, Muskingum routing, Muskingum–Cunge routing, and Straddle Stagger routing are used (Im *et al.* 2003). The meteorological model consists of different methods like frequency storm, gauge weights, gridded precipitation, inverse distance, HMR52, SCS storm, specified hyetograph, and the standard project storm.

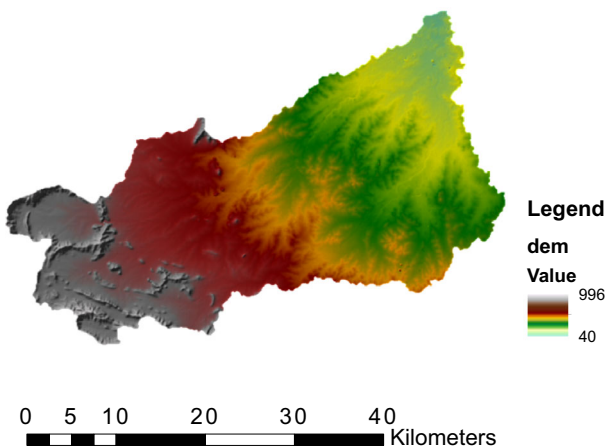


Figure 5. DEM of the study area – Koraiyar basin.

3.6 Modelling method

The basin model consists of hydrologic elements like sub-basin, reach, junction, sink, source, and diversions. The DEM data is imported into ArcGIS to delineate the basin. Terrain processing methods by GIS help to create the sub-basin and basin. The land-use and Curve Number maps are created to assign *CN* values to each sub-basin. The weighted *CN* values are calculated for each sub-basin with the averaging method and given as input to all the sub-basin models.

The meteorological model is provided with the rainfall data that is connected with all sub-basins. The control specification model consists of start and stop time, date, and duration time steps for simulation at various time intervals. The dataset for each model is imported, and then the hydrologic simulation is completed by using the dataset for the basin, precipitation quantum, and the control specification model. SCS-CN techniques are used to analyze the land-use land-cover changes and runoff losses. The SCS-Unit hydrograph method is used for transformation, and the Muskingum method is used for flood routing. The maximum rainfall event is given as input to the HEC-HMS model. The flood hydrograph and peak discharge are determined for maximum rainfall events. According to Ramakrishnan *et al.* (2009), the SCS-CN method can be adopted in places of limited data availability. The SCS-CN loss model is used in the present study due to limited available data, which estimates precipitation excess as a function of cumulative precipitation, soil cover, and land use, as given in the following (equation 1).

$$P_e = \frac{(p - I_a)^2}{(P - I_a + S)}, \quad (1)$$

where P_e is the accumulated precipitation excess at time t , P is accumulated rainfall depth at time t , I_a is the initial abstraction (initial loss), and S is potential maximum retention given in equation (3), a measure of the ability of a watershed to abstract and retains storm precipitation. The SCS develops an empirical relationship between I_a and S as $I_a = 0.2S$. Therefore, the cumulative excess at time t is given using equation (2).

$$P_e = \frac{(p - 0.2s)^2}{(P - 0.8 + S)}, \quad (2)$$

$$S = \frac{25400 - 254CN}{CN} \quad (3)$$

The parameter which influences land-use land-cover and soil type is the SCS curve number, which is calculated from collected and overlapped data of land use and hydrologic soil groups (USDA 1972; Merwade 2010). Here, CN is the SCS curve number, which represents the combination of a hydrologic soil group and land-use classes in this study. The SCS curve number method is used to simulate the hydrologic loss rate, and the SCS unit hydrograph method is used to calculate the runoff rate. The simulating process is carried out by using a specified storm hyetograph for the meteorological model. In control specification, the start and end time are given for model simulation at various intervals.

The Muskingum method is adopted for channel routing in this study according to Chu and Chang (2009), and the equation (4) adopted is shown below.

$$Q_2 = (c_1 - c_2)I_1 + (1 - c_1)Q_1 + c_2I_2 \quad (4)$$

$$c_1 = \frac{2 * \Delta t}{2 * K * (1 - X) + \Delta t} \quad (5)$$

$$c_2 = \frac{\Delta t - 2 * K * X}{2 * K * (1 - X) + \Delta t} \quad (6)$$

I_1 and I_2 represent inflow to the routing at the beginning and end of computation intervals, and Q_1 and Q_2 represent outflow from routing at the beginning and end of computation intervals, respectively. K represents travel time through reach, X is the Muskingum weighing factor that ranges from (0 to 0.5), Δt is the length of computation interval, and C_1 and C_2 are coefficients given in equations (5 and 6).

3.6.1 Basin model

The model is developed for the study area, and the basin is sub-divided into 27 sub-basins, as shown in figure 6. The hydrological parameters generated for all sub-basins of the Koraiyar basin are shown in table 1.

3.6.2 Transform method

The conversion of surplus rainfall to runoff is accomplished using the specified hyetograph method. The reason for adopting the SCS unit hydrograph method is because it requires only one parameter for each sub-basin in the lag time. The standard lag is known as the length of time

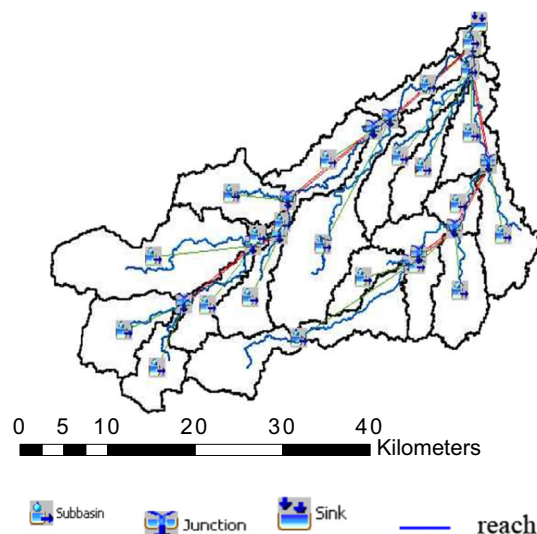


Figure 6. HEC-HMS hydrologic model for the Koraiyar basin.

between the centroid of precipitation mass and the peak discharges of the resulting hydrograph (USGS 2012). In the transform method, the lag time is given as input, and the SCS developed is given as a link between the time of concentration (T_c) and the lag time (T_{lag}), as given by equation (7). It is calculated by 0.6 times of concentration by using equation (8).

$$T_{lag} = \frac{L^{0.8}(S + 1)^{0.7}}{1900\sqrt{Y}}, \quad (7)$$

L is the most extended watercourse length in the watershed (m), S is the potential maximum retention (mm), and Y is an average watershed slope in %. Where T_c is the time of concentration in mins.

$$T_{lag} = 0.6 \times T_c. \quad (8)$$

3.6.3 Exponential recession constant

The exponential recession method was used to calculate the basic flow as shown in equation (9). The basic flow is an important parameter in runoff estimation as it defines the minimum river depth over which additional runoff accumulates (Knebl et al. 2005; Yuan et al. 2019).

$$Q_t = Q_0^{Rt}, \quad (9)$$

where Q_t is the threshold flow at time t calculated from observed flow hydrograph at recession limb expressed by straight line, R is exponential decay

Table 1. Parameters generated for sub-basins in Koraiyar watershed.

Sub-basin ID	Slope	Longest flow path	I_a	CN	T_c	T_{lag}	Recession constant value
W280	8.9	3.7	15.7	76.41	1.19	0.71	0
W300	8.2	3.1	13.3	79.21	0.92	0.55	0
W310	10.5	0.4	4.4	92	0.12	0.07	0
W370	7.9	2.9	11.5	81.6	0.78	0.47	0
W320	7.4	19.5	11.5	81.6	3.51	2.11	0
W330	7.4	15.4	10.6	82.67	2.82	1.69	0
W340	7.8	14.8	11.3	81.74	2.88	1.73	0
W400	9.6	11.8	14.2	78.15	2.99	1.79	0
W390	7.5	11.4	12.5	80.21	2.41	1.45	0
W420	7.4	12.0	10.7	82.61	2.30	1.38	0
W410	7.2	6.1	15.3	76.81	1.59	0.95	0
W460	8.1	4.7	12.1	80.81	1.22	0.73	0
W430	7.9	9.4	11.7	81.32	2.06	1.23	0
W510	8.5	4.2	10.9	82.29	1.08	0.65	0
W470	14.8	25.5	16.8	75.2	7.50	4.50	0
W360	8.6	33.0	11.9	81.05	5.88	3.53	0
W450	9.7	7.5	14.1	78.29	2.09	1.25	0
W440	7.9	8.8	11.0	82.26	1.87	1.12	0
W480	12.5	16.6	14.4	77.92	4.52	2.71	0
W530	18.1	11.6	23.6	68.32	5.35	3.21	0
W540	21.5	10.6	97.0	34.37	13.21	7.92	0
W520	11.0	34.8	14.5	77.77	7.70	4.62	0

constant and estimated from observed flow hydrograph, a dependent source of basic flow. Q_0 is initial base flow at time.

3.6.4 Meteorological model

The specified storm hyetograph method is used to produce artificial storm from statistical precipitation data in HEC-HMS model. This method aims to produce a specified storm hyetograph from the rainfall data obtained at various precipitation gauges. The partial or annual duration was used for developing precipitation depth-duration data for the selected single extreme rainfall events. In this method, the collected rainfall data is given as input for whole precipitation gauges present in the sub-basin to produce a hyetograph. The maximum rainfall events that occurred in the basin are given as input to the model. The rainfall data given, assumed as uniformly distributed, is due to presence of only one rain gauge station in the basin. The maximum average rainfall that occurred in the basin is shown in figure 7 and the maximum single events rainfall that occurred during 1976–2016 period is shown in table 2.

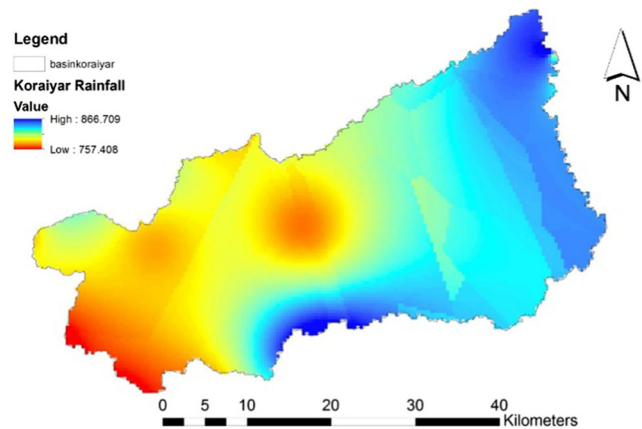


Figure 7. Spatial distribution of rainfall in Koraiyar basin.

3.7 Model conceptualization through HEC-HMS process

The HEC-HMS model is calibrated and evaluated for accuracy using calculated and observed streamflow data of the basin. The primary objective of the model calibration is to match the observed and calculated values with changed meteorological and land-cover conditions. Two evaluation criteria, correlation coefficient (R), and model efficiency (E) (Nash and Sutcliffe 1970) are

Table 2. Maximum single rainfall events that occurred in the basin (1976–2016).

Basin	Years	Month and date	RF max intensity	No. of rainy days
Koraiyar	1976	6-Nov	114.00	49
	1978	4-Nov	189.00	65
	1981	12-Sep	123.80	87
	1983	24-Dec	115.00	69
	1991	14-Sep	119.00	62
	1997	7-Nov	101.90	35
	1999	22-Nov	310.50	83
	2000	30-Jul	112.20	83
	2004	4-May	109.40	56
	2005	24-Sep	157.80	76
	2006	21-Aug	83.60	50
	2007	19-Dec	172.60	47
	2008	28-Nov	154.80	47
	2010	29-Nov	106.40	57
	2012	11-May	100.60	51
	2013	17-Nov	142.40	54

used to assess the model performance. The calibration and validation of the model are done for the maximum rainfall events of the past 40 years (1976–2016) of streamflow and precipitation data considered in this study. During model calibration, the hydrologic parameters and maximum rainfall events are used for the simulation. With the existing land-use data and rainfall data of more than 100 mm in a single day, almost over 16 maximum rainfall events are identified during 1976–2016 are used for the simulation. The initial abstraction, time of concentration, Muskingum factor, and travel time are the parameters considered in the model calibration process. The sequence of model parameters is estimated using an automated optimization tool provided by HEC-HMS by choosing specific objective functions.

The model efficiency (E) for the entire calibration period is computed for all the parameters to analyze the calibration results. The calibrated parameters are obtained by using peak-weighted root mean square error as the objective function as shown in equations (10–11).

$$\text{PWRMSE} = \sqrt{\frac{\sum_{t=1}^N (Q_{ot} - Q_{st}) \frac{Q_{ot} + Q_{ave}}{2Q_{ave}}}{N}} \quad (10)$$

$$Q_{ave} = \frac{1}{N} \sum_{t=1}^N Q_{ot}. \quad (11)$$

Finally, the validation is performed by using the parameters from the calibration process, which are

not changed during model validation. The HEC-HMS model is calibrated by using rainfall data from the selected extreme rainfall years of 4th Nov 1978 to 7th Nov 1997. Similarly, the validation was carried from the maximum rainfall event from 30th Jul 2000 to 17th Nov 2013. Out of 16 maximum single rainfall events, the maximum rainfall that occurred within these events is around 310.55 mm on 22nd Nov 1999, where the model calibration and validation is adopted before and after this event. The calibration parameters for single event simulation and the optimized parameter sets for each calibrated flood event are obtained by selecting peak weighted root mean square error as the objective function by using Nelder and Mead simplex search algorithm provided by HEC-HMS.

The reason for considering the extreme rainfall event of 22nd Nov 1999 is that Koraiyar River basin does not have continuous flow measurements and it is the only measured extreme flood event among these events. Hence the model calibration and validation is carried with respect to the 1999 flood event measured at the outlet of the basin. From the observed event, it is clear that there is some difference in the peak of simulated and observed peak flow. For all these events, the peak discharge is compared and verified with the maximum event that occurred in the basin. From the analysis, the time to peak, peak inflow and volume of inflow are completely different in all these events are due to rainfall fluctuations and unaccounted surface runoff from the nearby urban regions that joins the Koraiyar river in downstream.

4. Results and discussions

4.1 Simulation of HEC-HMS for single event simulation

The percentage error in volume (PEV) in the HEC-HMS model specifies that the simulated discharge may be above or below the measured values. The ideal value of PEV is 0. The +ve value of PEV shows that the model has less estimated streamflow, whereas negative value shows high estimation. The PEV values within 10% are considered very good, 10–15% good, 15–25% satisfactory and unsatisfactory above 25% (Moriassi *et al.* 2007). The relative peak error flow during 1977–2016 in the basin ranges from –17.8% to 3%. The simulated mean annual runoff is around 95.1 mm, with the relative peak flow volume error of –14.3% to 0.11%, respectively. The initial abstractions of all sub-basins range from 97.0 to 4.4, and during the calibration period, it is optimized automatically. The maximum values obtained after optimization of initial abstraction are in the range of 11.47–54.96. After the optimization process, the parameter values for each sub-basin range around 11.47, 19.70, 32.29, and 54.96 mm. The Nash Sutcliff values obtained during model calibration range from 0.5 to 0.6, is shown in figure 8 except for the year 1976. If the NSE value is around 1, it indicates the best fit between simulated and observed hydrographs. The results obtained show that the model performance is satisfactory during both calibration and validation periods, suggesting that the selected model from HEC-HMS can be applied to the Koraiyar basin for runoff simulations.

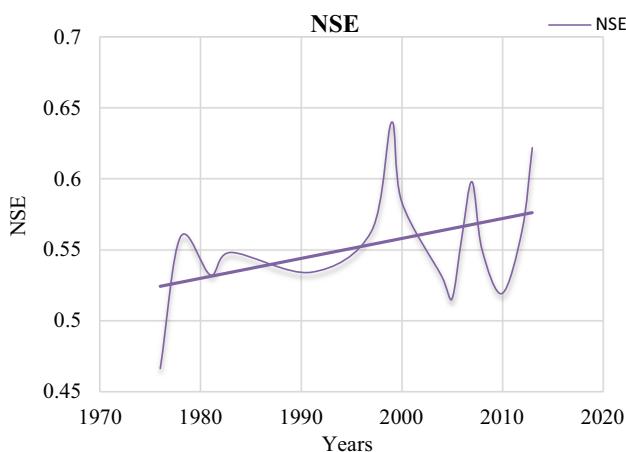


Figure 8. Graphical plot of NSE values.

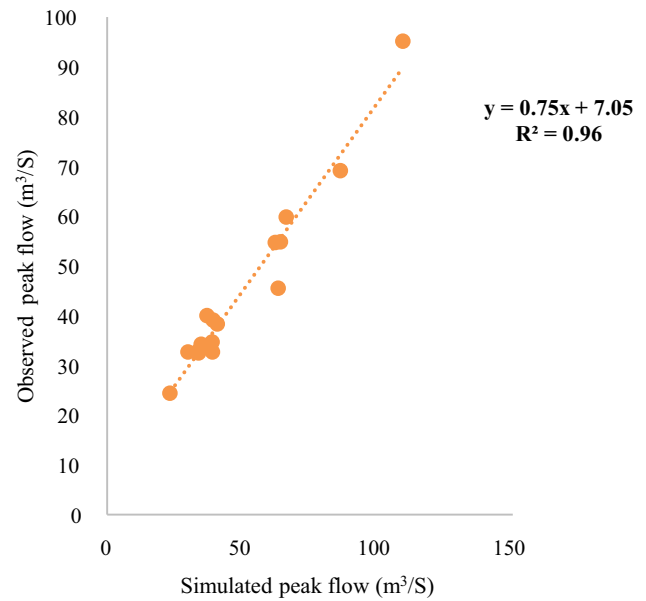


Figure 9. Regression for peak flood flow in m^3/s (1976–2016).

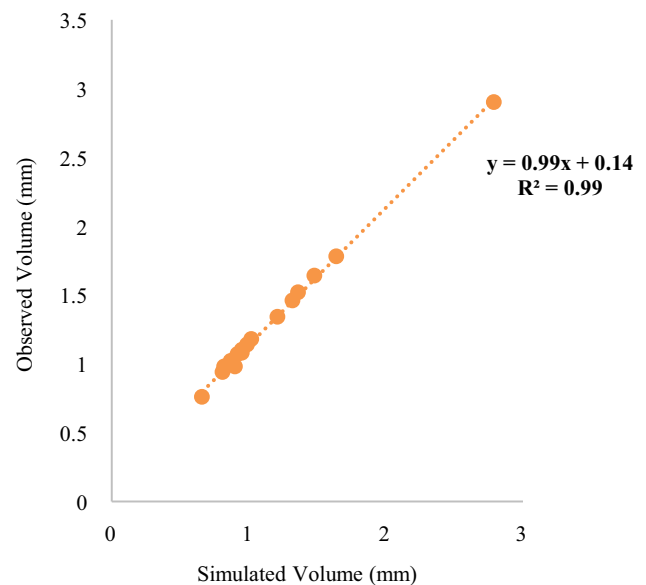


Figure 10. Regression for peak flood volume in mm (1976–2016).

The simulated and observed peak flood flow and volume of these 16 events that occurred between 1976 and 2013 show a good correlation coefficient with the regression values of $R^2 = 0.96$ and 0.99 , as shown in figures 9 and 10. The results obtained show that the model performance is satisfactory during both calibration and validation periods, suggesting that the selected model from HEC-HMS will be useful for runoff simulations in the Koraiyar basin.

Table 3. Sensitivity analysis of initial abstraction and curve number for calibrating flood simulation by daily time-step.

Process of simulation	Flood no. Date and year	Observed peak flow (m^3/s)	Simulated peak flow (m^3/s)	Observed flood volume (mm)	Simulated flood volume (mm)	Relative peak flow error (%)	Relative flood volume error (%)	Nash	SCS CN	Optimized I_a
Calibration	6-Nov-1976	63.3	45.5	0.95	1.08	-17.8	0.14	0.466	0.01	19.74
	4-Nov-1978	66.2	59.8	1.64	1.78	-6.4	0.14	0.559	0.01	32.29
	12-Sep-1981	29.9	32.7	1.02	1.18	2.8	0.16	0.532	0.01	32.29
	24-Dec-1983	34.8	34.2	0.95	1.1	-0.6	0.14	0.548	0.01	19.74
	14-Sep-1991	40.8	38.3	0.99	1.14	-2.5	0.15	0.534	0.01	19.74
	7-Nov-1997	33.7	32.9	0.822	0.98	-0.8	0.16	0.563	0.01	19.74
	22-Nov-1999	109.4	95.1	2.79	2.9	-14.3	0.11	0.64	0.01	54.96

4.2 Sensitivity analysis of HEC-HMS for simulation of flood events

A sensitivity analysis is required to identify which parameter has much influence on the model output with respect to the change of parameter values. This technique is useful for complex hydrological models which has a large number of parameters (Liu and Sun 2010). In addition, it is necessary for an ungauged basin to identify the local controlling parameters. The calibrated parameter values of all the sub-basins for runoff simulation show that the average value of Muskingum travel time is between 0.5 and 1, and the weighting factor of each sub-basin is around 0.3 because the travel time of flood events is shorter and hence the weighting factor is kept smaller. The calibration and validation results for the runoff are listed in tables 3 and 4. The calibrated comparison between the observed and simulated discharge hydrograph for single rainfall events is shown in figure 11. In calibrated events, minimum initial loss, constant loss rate and recession constant values were also considered. The main motive of tuning these parameters is to increase the sensitivity of the model by setting high CN values. Such adjustments provide the best possible results for the validation events.

For model validation, optimized parameters were input and the model was run for nine other rainfall events. Comparison of simulated and observed discharges for these events has been presented in figure 12. The model estimated the observed flows quite reasonably for the validation phase.

It is noted that the simulated flood hydrograph shows closer values with the observed hydrographs for most rainfall-runoff events, except during the years 1978 and 2004. The overall comparison of flood hydrographs for calibrated and validated extreme event is shown in figures 13 and 14. The relative error of the simulated peak flow and flood volume is almost below 1% for most of the events except for the year 2013, which has a value of 3%. The mean simulated flood volume is 0.76%, and for other events, it ranges between 1.08 and 1.78%. In the flood hydrographs developed, efficiency observed in the year 1996 is 0.76. In the year 1999, a correlation of coefficient value of 2.9 was obtained, which is higher than the values obtained from other flood hydrographs.

The calibrated model shows the simulated and observed peak discharges out of 16 rainfall events, out of which seven events show differences between

Table 4. Sensitivity analysis of initial abstraction and curve number for validating flood simulation by daily time-step.

Process of simulation	Flood no. Date and year	Observed		Simulated		Relative		Relative		SCS CN	Optimized I_a
		peak flow (m^3/s)	flood volume (mm)	peak flow (m^3/s)	flood volume (mm)	peak flow error (%)	flood volume error (%)	Nash			
Validation	30-Jul-2000	39.2	0.92	39.1	1.07	-0.1	0.14	0.584	0.01	19.7	
	4-May-2004	39	0.9	32.7	0.98	-6.3	0.08	0.531	0.01	11.47	
	24-Sep-2005	86.3	1.36	69.1	1.52	-17.2	0.16	0.515	0.01	32.22	
	21-Aug-2006	23.3	0.66	24.4	0.76	1.1	0.11	0.559	0.01	11.47	
	9-Dec-2007	62.2	1.48	54.7	1.64	-7.5	0.16	0.598	0.01	32.29	
	11-May-2008	64.1	1.32	54.8	1.46	-0.93	0.15	0.55	0.01	32.29	
	28-Nov-2010	38.9	0.87	34.7	1.02	-4.2	0.16	0.519	0.01	19.70	
	29-Nov-2012	33.8	0.81	32.5	0.94	-1.3	0.13	0.564	0	19.70	
	17-Nov-2013	37	1.21	40	1.34	3	0.13	0.622	0.01	32.29	

simulated and observed discharges. The year 1999 is recorded as the year which had the highest rainfall event (on 22nd November 1999) and shows a difference of -14.3% in peak flow.

Similarly, the other six events also show differences, and this might be due to rainfall season, time of travel, and topographic condition. On 4th May 2004, the simulated flow has a value of 86.3 m^3/s and observed flow value of 69.1 m^3/s ; this shows the big difference between the simulated and observed flow. Similarly, the 11th May 2008, rainfall event also showed many differences in simulation and observation; this might be due to the event occurring in the summer season and initial abstraction in the flow. There are also differences in time of peak flow, and almost all simulated and observed events have differences of 1–1.5 h, as shown in table 5. The 12th September 1981 rainfall event shows a difference of 3 h, which is due to the travel time of peak flow.

In this study, the annual runoff is simulated for the CN and I_a which is optimized by Nelder–Mead simplex methods by trial values from 0 to 100 with 100 iterations. The initial loss, constant loss rate and recession constant values are also considered with this iterations as shown in table 6. The recession constant values are in the range of 0.5–0.6. These tunings were done to keep losses at lesser limit and to increase the sensitivity of model by considering the base flow contributions by high recession constant values. The impact and sensitivity of flood changes due to impervious factors are also considered by changing impervious from 1% to 1.5%; because of the study location’s rural nature and the sensitivity of flood occurrence due to increase in impervious surface, it is not considered as an influential factor in this study.

The parameters were analyzed during the calibration processes to make the best fit between observed and simulated values. This calibration was executed by applying different CN in the HEC-HMS simulated model. The HEC-HMS offers automated and manual calibration. In this study, the automated calibration procedure was used. The changes in CN and initial abstraction play a prominent role in this basin and are optimized by several trial-and-error methods by 100 iterations, which show that they have a significant influence in the studied basin. In the future, the parameters like initial loss, constant loss rate storage coefficient recession constant and CN will be manually adjusted, and parameters which have more

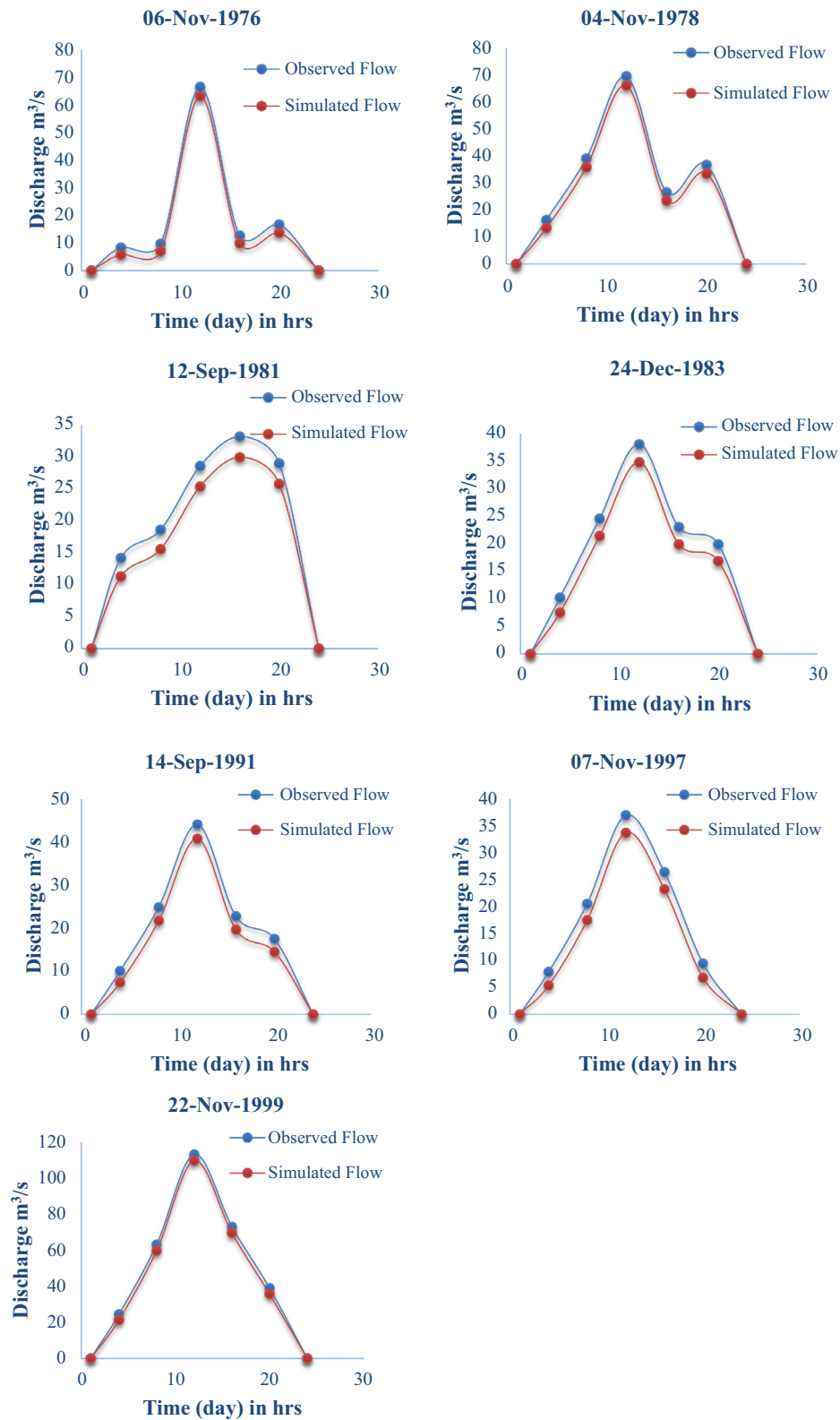


Figure 11. Comparison of observed and simulated flow of calibrated maximum rainfall events in the basin.

influence in the basin will be identified for more preciseness. The peak runoff obtained will be given as input to the HEC-RAS model for generating

flood plain maps for various flood events. The maximum flood spread area will be identified for the basin, and suitable flood mitigation measures

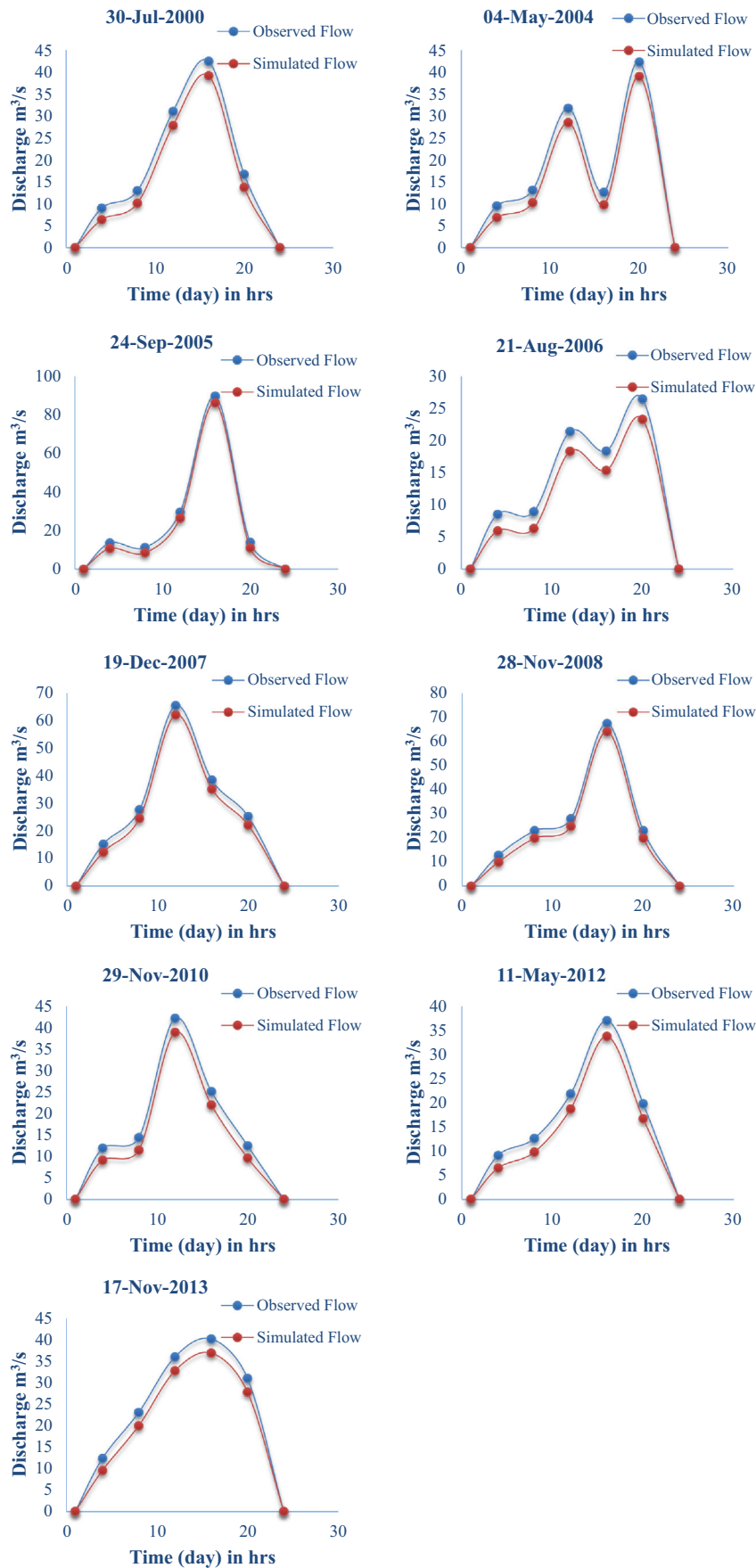


Figure 12. Comparison of observed and simulated flow of validated maximum rainfall events in the basin.

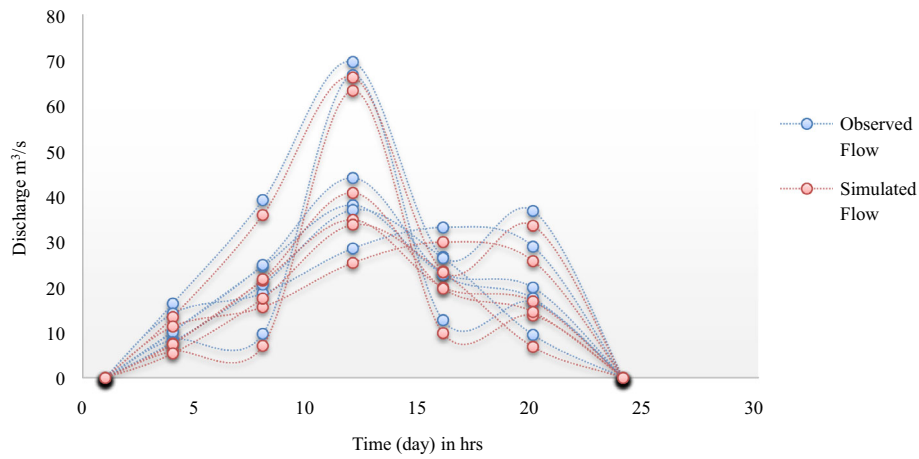


Figure 13. Calibrated flood hydrographs of selected extreme events from (1976–1997).

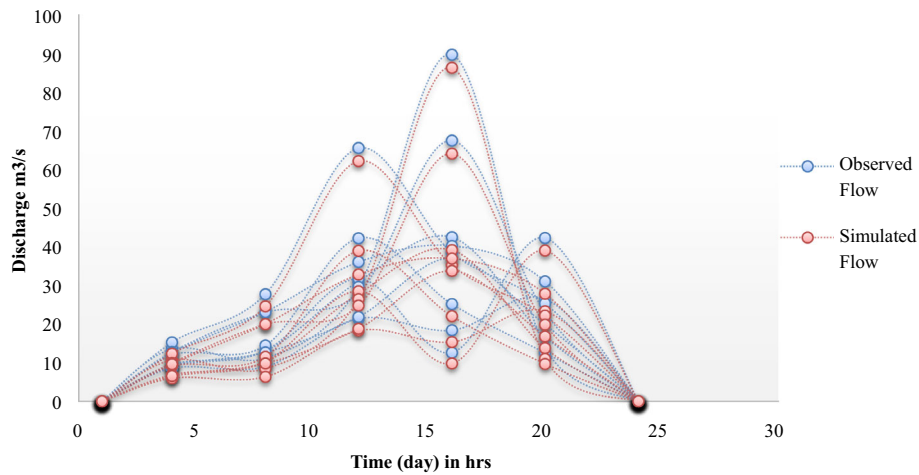


Figure 14. Validated flood hydrographs of selected extreme events from (2000–2013).

Table 5. *Simulated and observed time of peak.*

Date-Month-Year	Simulated		Observed		Relative peak flow error (%)
	Start time (h)	End time (h)	Start time (h)	End time (h)	
6-Nov-1976	13:15	14:39	12:00	12:45	-18.8
4-Nov-1978	13:15	14:22	12:00	12:38	-7.4
12-Sep-1981	19:00	15:01	16:00	13:36	4.8
24-Dec-1983	13:30	14:26	12:00	12:41	1.6
14-Sep-1991	13:30	14:20	12:00	12:28	-1.5
7-Nov-1997	14:30	14:23	12:00	12:05	-1.8
22-Nov-1999	14:00	14:29	12:00	12:30	-15.3
30-Jul-2000	17:00	15:30	16:00	13:48	-1.1
4-May-2004	21:00	15:44	20:00	14:42	-5.3
24-Sep-2005	17:15	16:03	16:00	14:11	-16.2
21-Aug-2006	20:45	15:40	20:00	14:30	1.5
19-Dec-2007	14:00	14:37	12:00	12:46	-8.5
28-Nov-2008	17:15	15:34	16:00	13:51	-1.93
29-Nov-2010	14:30	14:25	12:00	12:30	-4.5
11-May-2012	17:15	15:36	16:00	14:04	-2.3
17-Nov-2013	17:00	15:15	16:00	13:40	3.5

Table 6. *Calibrated results for each sub-basin in Koraiyar basin.*

Sub-basin ID	I_a	CN	K	x	Recession constant value
W280	19.71	77.1	0.35	0.26	0.50
W300	19.54	80.1	0.36	0.25	0.51
W310	11.5	93.8	0.35	0.25	0.56
W370	19.35	82.88	0.35	0.26	0.71
W320	19.35	82.51	0.36	0.25	0.50
W330	19.36	83.92	0.36	0.25	0.52
W340	19.36	82.85	0.35	0.25	0.61
W400	19.78	79.14	0.35	0.24	0.62
W390	19.68	81.89	0.36	0.24	0.58
W420	19.24	83.11	0.36	0.26	0.54
W410	19.78	77.02	0.35	0.24	0.53
W460	19.70	81.22	0.34	0.24	0.55
W430	19.65	82.45	0.35	0.24	0.59
W510	19.48	83.35	0.32	0.26	0.59
W470	19.78	76.20	0.36	0.25	0.55
W360	19.78	82.65	0.35	0.25	0.56
W450	19.78	79.14	0.36	0.24	0.54
W440	19.46	83.76	0.31	0.25	0.54
W480	19.75	78.12	0.36	0.26	0.53
W530	33.42	69.25	0.32	0.26	0.54
W540	53.96	35.38	0.38	0.26	0.53
W520	32.22	78.98	0.31	0.24	0.52

will be taken for the basin based on its flood-carrying capacity.

5. Conclusion

In the present work, DEM data of 30 m resolution is used for delineation of the Koraiyar basin and its catchment characteristics by using Arc Hydro extension in ArcGIS. The soil and land-use land-cover data are used to analyze the influence of runoff characteristics in the basin. This study also describes a methodology to calibrate and evaluate the open source data based model for runoff simulations for single extreme rainfall events for which the model can predict any peak flows or flood location in real time before or during a rainfall event.

The HEC-HMS hydrologic modelling software is adopted in the basin to predict the surface runoff. The SCS curve number loss method is used to define the hydrologic losses in the basin, and the SCS unit hydrograph method is used for effective rainfall transformation. The model parameters are calibrated and validated against the measured peak runoff event that happened before and after on 22nd November 1999. There was consistency

between simulated and observed flows with percent difference in volume and percent difference in peak flows in the range of 0.5–0.6. The Nash and Sutcliffe efficiency (NSE) is used to estimate the goodness-of-fit between the observed and modelled streamflow. From the study, it is observed that the model adopted was well capable of simulating the hydrologic response of the Koraiyar basin for the extreme rainfall event. The runoff values for individual ungauged sub-basins are also predicted in Koraiyar basin which might be taken as noteworthy point in this study, for estimations in ungauged basins.

Further the model performance can be improved by more amount of observed data in the basin which may provide further insight into the hydrology of the basin for further studies. The results obtained nearly match the run-off generated from the specified hyetograph, and the method is therefore used for flood hazard and risk assessment of the Koraiyar basin by using HEC-RAS. The area is an ungauged river basin located in Tiruchirappalli city, and the current methodology adopted can be used in the estimation of the runoff in other areas with similar land conditions. The rainfall–runoff outputs from HEC-HMS model can be used in hydraulic models for flood estimation and

in early flood warning studies. This modelling approach can also be used by hydrologist for better flood risk assessment in ungauged basins.

Acknowledgements

The authors gratefully acknowledge the State Surface and Groundwater Data Centre, Chennai, and Irrigation Management Training Institute for providing rainfall data, Tiruchirappalli. The authors also extend their thanks to USGS, SRTM website for providing Remote Sensing Images freely available. The US Army Corps of Engineers were appreciated for providing HEC-HMS and HEC-RAS is open-source software. Finally, to the Editor of this journal, the reviewers for making much effort to review the manuscripts and their team for their great support during the review of the submitted manuscript.

Authors statement

The first author Surendar Natarajan contributed in this study by data collection, framed methodology of the study, analysis, results and preparation of manuscript. The results and manuscript were reviewed and corrected by second author Nisha Radhakrishnan.

References

- Ali M, Khan S J, Aslam I and Khan Z 2011 Simulation of the impacts of land-use change on surface runoff of Lai Nullah Basin in Islamabad, Pakistan; *Landscape Urban Plan.* **102** 271–279.
- Anandharuban P, Rocca M L and Elango L 2019 A box-model approach for reservoir operation during extreme rainfall events: A case study; *J. Earth Syst. Sci.* **128(229)** 1–14, <https://doi.org/10.1007/s12040-019-1258-7>.
- Apel H, Aronica G T, Kreibich H and Thielen A H 2009 Flood risk analyses – how detailed do we need to be?; *Nat. Hazards* **49** 79–98.
- Aryal *et al.* 2020 A model-based flood hazard mapping on the southern slope of Himalaya; *Water* **12** 540, <https://doi.org/10.3390/w12020540>.
- Azama M, Kimb H S and Maenga S J 2017 Development of food alert application in Mushim stream watershed Korea; *Int. J. Disaster Risk Reduct.* **21** 11–26.
- Bates P D 2004 Remote sensing and flood inundation modeling; *Hydrol. Process.* **18** 2593–2597.
- Bhaskar N R 1988 Projection of urbanization effects on runoff using Clark's instantaneous unit hydrograph parameters; *Water Resour. Bull.* **24(1)** 113–124.
- Cheng S J and Wang R Y 2002 An approach for evaluating the hydrological effects of urbanization and its application; *Hydrol. Process.* **16** 1403–1418.
- Chu H J and Chang L C 2009 Applying particle swarm optimization to parameter estimation of the nonlinear muskingum model; *J. Hydrol. Eng.* **14** 1024–1027.
- Dhruvesh P P and Prashant K S 2013 Flood hazards mitigation analysis using remote sensing and GIS: Correspondence with Town Planning Scheme; *Water Resour. Manag.* **27** 2353–2368.
- Eyad A and Broder M 2013 Modelling rainfall runoff relations using HEC-HMS and IHACRES for a single rain event in an arid region of Jordan; *Water Resour. Manag.* **27** 2391–2409, <https://doi.org/10.1007/s11269-013-0293-4>.
- Ferguson B K and Suckling P W 1990 Changing rainfall–runoff relationships in the urbanizing Peachtree Creek watershed, Atlanta, Georgia; *Water Resour. Bull.* **26(2)** 313–322.
- Hapuarachchi H A P, Wang Q J and Pagano T C 2011 A review of advances in flash flood forecasting; *Hydrol. Process.* **25** 2771–2784, <http://dx.doi.org/10.1002/hyp.8040>.
- Huang H J, Cheng S J, Wen J C and Lee J H 2008 Effect of growing watershed imperviousness on hydrograph parameters and peak discharge; *Hydrol. Process.* **22(13)** 2075–2085.
- Im S, Brannan K M and Mostaghimi S 2003 Simulating hydrologic and water quality impacts in an urbanizing watershed; *J. Am. Water Resour. Assoc.* **39** 1465–1479.
- Ismail E 2015 Flash flood hazard mapping using satellite images and GIS tools: A case study of Najran City, Kingdom of Saudi Arabia (KSA); *Egyptian J. Remote Sens. Space Sci.* **18** 261–278.
- Jakeman A J and Hornberger G M 1993 How much complexity is warranted in a rainfall–runoff model?; *Water Resour. Res.* **29(8)** 2637–2649.
- Khatri H B, Jain M K and Jain S K 2018 Modelling of streamflow in snow dominated Budhigandaki catchment in Nepal; *J. Earth Syst. Sci.* **127** 100, <https://doi.org/10.1007/s12040-018-1005-5>.
- Kim E S and Choi H 2015 A method of flood severity assessment for predicting local flood hazards in small ungauged catchments; *Nat. Hazards* **78** 2017–2033.
- Knebl M R *et al.* 2005 Regional scale flood modelling using NEXRAD rainfall, GIS, and HEC-HMS/RAS: A case study for the San Antonio River Basin Summer 2002 storm event; *J. Environ. Manag.* **75** 325–336.
- Komuscu A U and Celik S 2012 Analysis of the Marmara flood in Turkey, 7–10 September 2009: An assessment from hydrometeorological perspective; *Nat. Hazards*, <https://doi.org/10.1007/s11069-012-0521-x>.
- Laouacheria F and Mansori R 2015 Comparison of WBNM and HEC-HMS for runoff hydrograph prediction in a small urban catchment; *Water Resour. Manag.* **29** 2485–2501, <https://doi.org/10.1007/s11269-015-0953-7>.
- Lastra J *et al.* 2008 Flood hazard delineation combining geomorphological and hydrological methods: An example in the Northern Iberian peninsula; *Nat. Hazards* **45** 277–293.
- Lillesand T M and Kiefer R W 2003 *Remote sensing and image interpretation*; New York: John Wiley and Sons.
- Liu Y and Sun F 2010 Sensitivity analysis and automatic calibration of a rainfall–runoff model using multi-objectives; *Ecol. Inf.* **5** 304–310.

- Madsen H 2000 Automatic Calibration of a conceptual rainfall-runoff model using multiple objectives; *J. Hydrol.* **235(3)** 276–288, [https://doi.org/10.1016/S0022-1694\(00\)00279-1](https://doi.org/10.1016/S0022-1694(00)00279-1).
- Maity R 2018 *Frequency analysis, risk, and uncertainty in hydroclimatic analysis*; *Stat. Methods Hydrol. Hydroclimatol.* 444p, <https://doi.org/10.1007/978-981-10-8779-0>.
- Matej V and Jana V 2016 Flood hazard and flood risk assessment at the local spatial scale: A case study; *Geomatics, Nat. Hazards and Risk* **7(6)** 1973–1992.
- Mehdi K, Alireza S and Bahram S 2018 Loss of life estimation due to flash floods in residential areas using a regional model; *Water Resour. Manag.* **32** 4575–4589.
- Merwade V 2010 *Creating SCS Curve Number Grid using HEC Geo HMS*; School of Civil Engineering, Purdue University, <http://web.ics.purdue.edu/~vmerwade/education/cngrid.pdf>.
- Moriasi D N, Arnold J G, Van Liew M W, Bingner R L, Harmel R D and Veith T L 2007 Model evaluation guidelines for systematic quantification of accuracy in watershed simulation; *Trans. ASABE* **50(3)** 885–900.
- Nash J E and Sutcliffe J E 1970 River flow forecasting through conceptual models. Part 1: A discussion of principles; *J. Hydrol.* **10** 282–290.
- Onusuel G, Nilgun H and Ali G 2010 A combined hydrologic and hydraulic modelling approach for testing efficiency of structural flood control measures; *Nat. Hazards* **54** 245–260.
- Pawan N B and Jayantilal N P 2018 Event-based rainfall-runoff modelling and uncertainty analysis for lower Tapi Basin, India; *ISH J. Hydraul. Eng.*, <https://doi.org/10.1080/09715010.2018.1464406>.
- Ramakrishnan D, Bandyopadhyay A and Kusuma K N 2009 SCS-CN and GIS-based approach for identifying potential water harvesting sites in the Kali Watershed, Mahi River Basin, India; *J. Earth Syst. Sci.* **118(4)** 355–368.
- Reddy A M 2002 *Text book of remote sensing and geographical information systems*; Saint John: B.S. Publications.
- Sampath D, Weerakoon S and Herath S 2015 HEC-HMS model for runoff simulation in a tropical catchment with intra-basin diversions case study of the Deduru Oya River Basin, Sri Lanka; *Engineer.* **48(01)** 1–9, <https://doi.org/10.4038/engineer.v48i1.6843>.
- Scharffenberg W and Fleming M 2010 Hydrologic modelling system HEC-HMS v32 user's manual; USACE/HEC, Davis.
- Sintayehu L G 2015 Application of the HEC-HMS model for runoff simulation of Upper Blue Nile River Basin; *Hydrol. Curr. Res.* **6(2)** 199, <https://doi.org/10.4172/2157-7587.1000199>.
- Surendar N and Nisha R 2019 Simulation of extreme event-based rainfall-runoff process of an urban catchment area using HEC-HMS; *Model. Earth Syst. Environ.* **5** 1867–1881, <https://doi.org/10.1007/s40808-019-00644-5>.
- Suribabu C R, Bhaskar J and Neelakantan T R 2012 Land use/cover change detection of Tiruchirapalli city, India using integrated remote sensing and GIS tools; *J. Indian Soc. Rem. Sens.* **40(4)** 699–708.
- Suribabu C R and Bhaskar J 2015 Evaluation of urban growth effects on surface runoff using SCS-CN method and Green-Ampt infiltration model; *Earth Sci. Inform.* **8** 609–626, <https://doi.org/10.1007/s12145-014-0193-z>.
- Tung Y K and Mays L W 1981 State variable model for urban rainfall-runoff process; *Water Resour. Bull.* **17(2)** 181–189.
- United States Army Corps of Engineers (USACE) 2008 Hydrological modelling system, HEC-HMS, user's manual, version 3.3; Davis, CA, USA.
- US Army Corps of Engineers (USACE) 2013 Hydrologic Engineering Centre: Hydrologic modelling system HEC-HMS, user's manual version 4; <http://www.hec.usace.army.mil/software/hec-geohms/downloads.aspx>.
- USDA 1972 *National engineering handbook, section 4, hydrology, soil conservation service*; US Government Printing Office, Washington, DC.
- USGS 2012 Estimating basin lag time and hydrograph timing indexes used to characterize storm flows for runoff-quality analysis; Scientific Investigations Report, Reston, Virginia, USA, U.S. Geological Survey, 58p.
- Xuefeng C and Steinman A 2009 Event and continuous hydrologic modelling with HEC-HMS; *J. Irrig. Drain. Eng.* **135 1(119)** 119–124, [https://doi.org/10.1061/\(asce\)0733-9437](https://doi.org/10.1061/(asce)0733-9437) (2009).
- Yang X L, Ren L L, Singh V P, Liu X F, Yuan F, Jiang S H and Yong B 2012 Impacts of land use and land cover changes on evapotranspiration and runoff at Shalamulun River watershed, China; *Hydrol. Res.* **43(1–2)** 23–37.
- Yuan W, Liu M and Wan F 2019 Calculation of critical rainfall for small-watershed flash floods based on the HEC-HMS hydrological model; *Water Resour. Manag.* **33** 2555–2575, <https://doi.org/10.1007/s11269-019-02257-0>.
- Yucel I 2015 Assessment of a flash flood event using different precipitation datasets; *Nat. Hazards* **79** 1889–1911.
- Yusop Z, Chan C H and Katimon A 2007 Runoff characteristics and application of HEC-HMS for modelling storm flow hydrograph in an oil palm catchment; *Water Sci. Technol.* **56** 41–48.
- Zafar S and Zaidi A 2015 Impact of urbanization on basin hydrology: A case study of the Malir Basin, Karachi, Pakistan; *Regional Environmental Change*, <https://doi.org/10.1007/s10113-019-01512-9>.
- Zaharia L, Costache R, Pravălie R and Minea G 2015 Assessment and mapping of flood potential in the Slănic catchment in Romania; *J. Earth Syst. Sci.* **124(6)** 1311–1324.
- Zhang H L, Wang Y J, Wang Y Q, Li Q D and Wang X K 2013 The effect of watershed scale on HEC-HMS calibrated parameters: A case study in the clear creek watershed in Iowa, US; *Hydrol. Earth Syst. Sci.* **17** 2735–2745.
- Zope P E, Eldho T I and Jothiprakash V 2015 Impacts of urbanization on flooding of a coastal urban catchment: A case study of Mumbai City, India; *Nat. Hazards* **75** 887–908.